 doi:10.20944/preprints202111.0255.v1

Article

Vibration Compensation for a Vehicle-mounted Atom Gravimeter

Jie Guo [1,2], Siqian Ma [2], Chao Zhou [2], Jixun Liu [2,*], Bin Wang [2,3], Debin Pan [1,2], and Haicen Mao [2,*]

[1] Wuhan National Laboratory for Optoelectronics, Huazhong University of Science and Technology, Wuhan 430074, People's Republic of China; guojiehust@foxmail.com (J.G.); pdb@gdjsxjs.onexmail (D.P.)
[2] Wuhan National Laboratory for Optoelectronics, Huazhong Institute of Electro-Optics, Wuhan 430223, People's Republic of China; masiqian@buaa.edu.cn (S.M.); gxmarble@163.com (C.Z.); hustwangbin@163.com (B.W.)
[3] University of Chinese Academy of Sciences, Beijing 430071, People's Republic of China
* Correspondence: liujixun@buaa.edu.cn (J.L.); mhaicen@qq.com (H.M.); Tel.: +86-27-5900-2300

Abstract: The performance of the absolute atom gravimeters used on moving platforms, such as vehicles, ships and aircrafts, is strongly affected by the vibration noise. To suppress its influence, we summarize a vibration compensation method utilizing data measured by a classical accelerometer. The measurements with the accelerometer show that the vibration noise in the vehicle can be 2 order of magnitude greater than that in the lab during daytime, and can induce an interferometric phase fluctuation with a standard deviation of 16.70π. With the compensation method, our vehicle-mounted atom gravimeter can work normally in these harsh conditions. Comparing the Allan standard deviations before and after the vibration noise correction, we find a suppression factor of 22.74 can be achieved in static condition with an interrogation time of T = 20 ms, resulting a sensitivity of 1.35 mGal/Hz$^{1/2}$, and a standard deviation of 0.5 mGal with an average time of 10 s. We also demonstrate the first test of an atom gravimeter in a moving vehicle, in which a suppression factor of 50.85 and a sensitivity of 60.88 mGal/Hz$^{1/2}$ were realized with T = 5 ms.

Keywords: atom gravimeter; vibration compensation; vehicle-mounted

1. Introduction

Gravimetry plays an important role in metrology, navigation, geodesy, geophysics [1, 2], etc. After M. Kasevich and S. Chu demonstrated the measurment of gravity with their atom interferometer using three Raman pulses in 1991 [3, 4], many institutes began to develop atom gravimeters that can be used outside laboratories with similar configurations. In recent years, AOSense, Inc. [5] and Muquans [6] have made atom gravimeters commercial available. With gravimeters developed by Muquans fixed at the measurement location, gravity measurement can reach μGal level [6]. Besides, atom gravimeters can also be used for absolute airborne and marine gravimetry, with mGal and submGal precisions respectively [7, 8].

Atom gravimeters are very sensitive to vibrations. Therefore, precision measurement of gravity cannot be performed without any suppression of vibration noise [9]. The suppression can be achieved with vibration-isolation systems, which can be passive [10] or active [11]. Another approach is to correct their impact on the gravity measurement by measuring them [12]. The vibration compensation technique has already been used by Muquans in their gravimeter [13]. As a result, their gravimeter is robust against seismic noise without the need of an isolation device [13].

To achieve vibration compensation, the vertical acceleration or velocity of the mirror for reflecting the Raman laser beam needs to be measured with an accelerometer [13, 14], seismometer [9, 12, 14] or laser interferometer [15]. Here a vibration compensation

method is summarized and demonstrated with our vehicle-mounted atom gravimeter, in which the acceleration of the mirror is measured with an accelerometer. To our knowledge, atom gravimeters have been tested in a stopped truck [1, 16], a moving ship [8] and an airplane in flight [7], but not in a moving vehicle. Our experiments were conducted in both static and dynamic conditions. The vibration noise levels and the suppression factors of the vibration compensation in these conditions are compared, which can provide supplementary information for developing atom gravimeters used on moving platforms.

2. Experimental Setup and Methods

2.1 Experimental Setup

The atom gravimeter is composed of a sensor head, a gyro-stabilized platform, a laser system and control electronics. Figure 1a shows the sensor head and the 2-axis gyro-stabilized platform. The platform can maintain the sensor head aligned with the gravitational acceleration with a precision of 0.02°, using an integrated inertial measurement system. The whole apparatus is installed in the vehicle shown in Figure 1b, which has a diesel engine.

(**a**) (**b**)

Figure 1. (a) The sensor head and the gyro-stabilized platform of the atom gravimeter; **(b)** The vehicle used in the experiments.

The schematic diagram of the sensor head is illustrated in Figure 2. A standard three-dimensional magneto-optical trap (3D MOT) cools and collects ~10^8 ^{87}Rb atoms released from a dispenser in 130 ms. The atoms are then further cooled down to 5 μK in an optical molasses. Afterwards, the cold atoms are released in free fall, and transferred to $|F=1, m_F=0\rangle$ by a 110 μs long microwave π pulse for state preparation. After several milliseconds, the π/2 – π –π/2 sequence of Raman laser pulses are applied to split, reflect and recombine the matter waves. At the bottom of the vacuum chamber, the interference signal of the atom interferometer is obtained by measuring the population of atoms in $|F=2\rangle$ and $|F=1\rangle$ with a fluorescence method. The photodiode (PD), together with a lens beside the chamber, is used for the fluorescence detection.

Preprints (www.preprints.org) | NOT PEER-REVIEWED | Posted: 15 November 2021 doi:10.20944/preprints202111.0255.v1

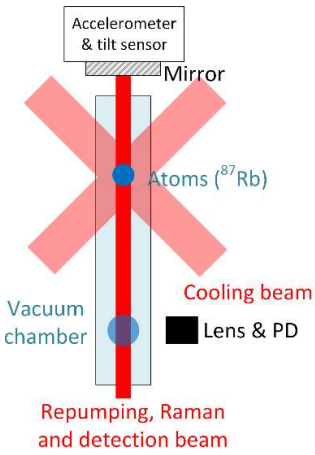

Figure 2. The schematic diagram of the sensor head.

After the Raman pulses, the proportion P of the atoms in $|F=2\rangle$ is given by [8]

$$P = P_m - \frac{C}{2}\cos\Phi, \tag{1}$$

where C is the contrast, P_m is the offset and Φ is the interferometric phase shift. The phase shift Φ can be written as

$$\Phi = (k_{eff} g - 2\pi\alpha)T^2 + \Phi_{vib}, \tag{2}$$

in which $k_{eff} = 4\pi/\lambda$ is the effective wave vector of the Raman beam, g is the gravitational acceleration, α is the frequency chirp applied to the Raman lasers to compensate the Doppler shift induced by gravity, Φ_{vib} is the phase shift induced by vibrations, and T is the time interval between the 3 Raman pulses, namely the interrogation time. With Equations (1) and (2), we are able to deduce g from P and Φ_{vib}.

2.2 Vibration Compensation Method

As shown in Figure 2, the Raman beam enter the vacuum chamber from the bottom. The vertical laser beam and its retro-reflection on the mirror mounted on the top of the chamber form the two counter-propagating Raman beams. The phase difference between the counter-propagating Raman beams is therefore defined by the position of the retro-reflection mirror [17]. A vertical displacement of this mirror by δz induces a Raman phase shift of $k_{eff}\delta z$ [14]. Therefore, the phase shift induced by vibrations of the mirror can be calculated with the following equation [9, 14]:

$$\Phi_{vib} = k_{eff}\int_{-\infty}^{\infty} g_s(t)v_z(t)dt, \tag{3}$$

where $v_z(t) = d\delta z/dt$ is the vertical velocity of the mirror, and $g_s(t)$ is the sensitivity function, given by [18]

$$g_s(t)=\begin{cases}0 & t<-2\tau-T\\ \sin(\Omega_{eff}(t+T)) & -2\tau-T\le t<-\tau-T\\ -1 & -\tau-T\le t<-\tau\\ \sin(\Omega_{eff}t) & -\tau\le t<\tau\\ 1 & \tau\le t<\tau+T\\ \sin(\Omega_{eff}(t-T)) & \tau+T\le t<2\tau+T\\ 0 & t\ge 2\tau+T\end{cases}, \quad (4)$$

where $\Omega_{eff}=\pi/(2\tau)$ is the effective Rabi frequency.

In our setup, we use an accelerometer (Nanometrics Titan Accelerometer) attached to the mirror to measure its vibrations. Since it measures the acceleration instead of the velocity, we need to change Equation (3) into the following form [19]:

$$\Phi_{vib}=k_{eff}\int_{-\infty}^{\infty}g_a(t)a_z(t)dt\,, \quad (5)$$

where $a_z(t)$ is the vertical acceleration of the mirror, and $g_a(t)$ is the acceleration sensitivity function. Comparing Equations (3) and (5), we find $g_a(t)$ can be expressed as

$$g_a(t)=\int_{-\infty}^{t}g_s(t)dt=\begin{cases}0 & t<-2\tau-T\\ \dfrac{\cos(\Omega_{eff}(t+T))+1}{\Omega_{eff}} & -2\tau-T\le t<-\tau-T\\ \dfrac{1}{\Omega_{eff}}+t+\tau+T & -\tau-T\le t<-\tau\\ \dfrac{1+\cos(\Omega_{eff}t)}{\Omega_{eff}}+T & -\tau\le t<\tau\\ \dfrac{1}{\Omega_{eff}}+\tau+T-t & \tau\le t<\tau+T\\ \dfrac{\cos(\Omega_{eff}(t-T))+1}{\Omega_{eff}} & \tau+T\le t<2\tau+T\\ 0 & t\ge 2\tau+T\end{cases}, \quad (6)$$

which is a triangle-like function. With Equations (5) and (6), we are able to apply a post-correction.

3. Results

3.1. Vibration Noise

To have a better knowledge of the vibration noise on the vehicle, we measured the vibrations in different places under several typical conditions, and made a comparison of their standard deviations in Table 1. The vibrations of the ground and the base plate are measured with a strong motion accelerograph (Nanometrics TitanSMA), in which the sample rate is 2 kHz. The base plate refers to the plate on the vehicle used to fix the gyro-stabilized platform. And the vibrations of the mirror are measured with the accelerometer used in the atom gravimeter, in which the sample rate is several tens of kilo-

Preprints (www.preprints.org) | NOT PEER-REVIEWED | Posted: 15 November 2021 doi:10.20944/preprints202111.0255.v1

hertz. The z axes of the accelerometer and the strong motion accelerograph are aligned with the gravitational acceleration.

Table 1. The standard deviations of vibrations in different places under several typical conditions.

Place	Speed (km/h)	σ_x (m/s²)	σ_y (m/s²)	σ_z (m/s²)
Ground in the lab (daytime)	/	0.0014	0.0011	0.0016
Base plate on the vehicle (engine off)	/	0.0084	0.0074	0.0063
Mirror in the sensor head (engine off)	/	0.0052	0.0054	0.0074
Base plate on the vehicle (engine on)	0	0.1381	0.0921	0.0449
Mirror in the sensor head (engine on)	0	0.0313	0.0257	0.0286
Mirror in the sensor head (engine on)	7	0.0394	0.0553	0.0888
Mirror in the sensor head (engine on)	40	0.1494	0.1018	0.1686

There are four typical conditions for the vehicle-mounted atom gravimeter. The first one refers to the case in which the engine of the vehicle is off. In this case, the gravimeter is powered up with the UPS. The vibrations are minimized which makes it possible to measure gravity with the longest interrogation time and the highest precision. However, the standard deviations of the vibrations in this case are still several times larger than those in the lab. The second one refers to the case in which the engine is on for generating electricity but the vehicle doesn't move. In this case the gravimeter can work for a much longer time. The platform together with the sensor head may significantly attenuate the vibrations induced by the engine. The third one refers to the case in which the vehicle moves with a speed of 7 km/h. In this case, the gravimeter can be used to measure gravity continuously along the path. The last one is the case in which the vehicle moves with a speed of 40 km/h, which is a typical speed for transportation. Obviously, the vibration noise on the vehicle can be nearly 1 or 2 order of magnitude greater than that in the lab, which makes the vibration compensation challenging. And the vibration noise in the 4th condition can be comparable with that in the aircraft used by R. Geiger et al. [19].

The influence of the vibration noise on the interferometric phase shift can be estimated from its power spectral density (PSD). According to [17], the rms standard deviation of the interferometric phase noise $\sigma_{\Phi_{vib}}^{rms}$ induced by vibrations can be evaluated by

$$(\sigma_{\Phi_{vib}}^{rms})^2 = \int_0^\infty |H(\omega)|^2 \frac{k_{eff}^2}{\omega^4} S_a(\omega) d\omega, \tag{7}$$

where $S_a(\omega)$ is the PSD of the vertical vibrations of the mirror. The phase transfer function $H(\omega)$ is given by [14, 17]

$$H(\omega) = \frac{4i\omega\Omega_{eff}}{\omega^2 - \Omega_{eff}^2} \sin\left(\frac{\omega(T+2\tau)}{2}\right)\left(\cos\left(\frac{\omega(T+2\tau)}{2}\right) + \frac{\Omega_{eff}}{\omega}\sin\left(\frac{\omega T}{2}\right)\right). \tag{8}$$

For the duration of our Raman pulses, the complex magnitude of the acceleration-transfer function $|H_a(2\pi f)| = k_{eff}|H(2\pi f)|/(2\pi f)^2$ versus the frequency f is displayed in Figure 3. Obviously, the function acts as a low pass filter.

Preprints (www.preprints.org) | NOT PEER-REVIEWED | Posted: 15 November 2021 doi:10.20944/preprints202111.0255.v1

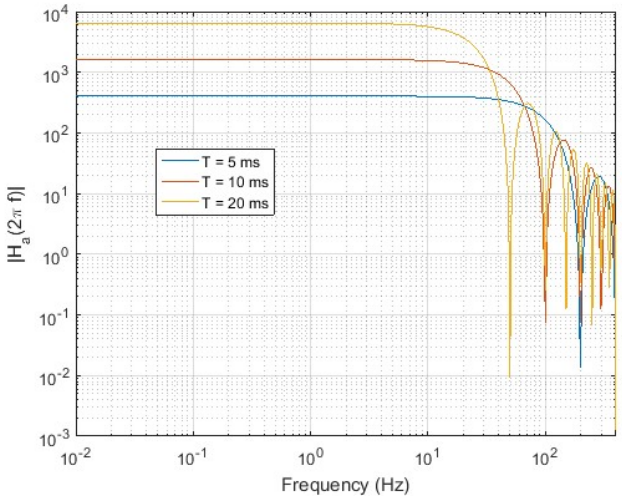

Figure 3. The complex magnitude of the acceleration-transfer function $|H_a(2\pi f)|$ versus the frequency f.

With the measured data, we calculated the square roots of the PSDs of the vertical vibrations of the mirror. Figure 4 shows the results obtained with the LPSD (for Logarithmic frequency axis Power Spectral Density) method [20, 21]. With these spectra and Equation (7), the influence of the vibration noise on the interferometric phase shift under the 4 typical conditions is estimated and shown in Table 2.

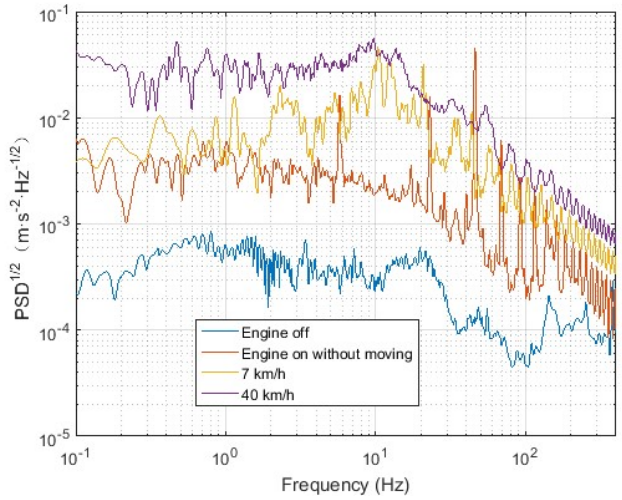

Figure 4. Square roots of the PSDs of vertical vibrations of the mirror under the four typical conditions.

Table 2. The rms standard deviation of the interferometric phase noise $\sigma_{\Phi_{vib}}^{rms}$ induced by vertical vibrations of the mirror under the 4 typical conditions. All the values are in radian.

	T = 5 ms	**T = 10ms**	**T = 20ms**
Engine off	0.29π	1.08π	3.57π
Engine on without moving	6.09π	15.41π	29.40π
7 km/h	10.80π	40.10π	133.96π

40 km/h	20.51π	76.41π	265.32π

The standard deviation of the phase noise for T = 5 ms induced by vibrations measured while the vehicle was moving with a speed of 7 km/h is over 10π, which is 2 times larger than the value for T = 20 ms in static condition while the engine was off, and more than an order of magnitude larger than the typical value for T = 60 ms in Muquans laboratory [13]. This makes the moving test challenging.

3.2. Vibration Noise Correction

In our experiments, the vibration noise was post corrected. The frequency chirp α applied to the Raman lasers was fixed. The interrogation time T is set to be 5 ms, 10 ms, or 20 ms, depending on the environmental conditions. Considering the z axes of the accelerometer might be misaligned with the Raman beam, the output signals along all its three axes were recorded by the control electronics of the atom gravimeter with a sample rate of 62.5 kHz. The data acquisition is therefore synchronized with the time sequence of the interferometer. A high pass filter, whose cut-off frequency is 0.03 Hz, is used to eliminate the bias of the accelerometer output. After the experiments were finished, we are able to calculate the phase induced by vibration with $\Phi_{vib} = \sum \eta_j \phi_{vib,j}$, where $j = x, y, z$ and $\phi_{vib,j} = k_{eff} \int_{-\infty}^{\infty} g_a(t - \tau_j) a_j(t) dt$ is the phase shift calculated from the accelerometer data along axis j [12]. The contribution η_j and delay τ_j along axis j, together with the fringe offset P_m and contrast C, can be determined by fringe fitting, in which the proportion P of the atoms in $|F = 2\rangle$ is the observed output and the accelerometer data are the input of the function.

The Allan standard deviation of the measured gravitational acceleration was calculated in order to evaluate the post correction. Figure 5 shows the results measured with the vehicle's engine off. After vibration noise correction, the standard deviation can reach 0.5 mGal with T = 20 ms and an average time of 10 s. Figure 6 shows the results measured with the vehicle's engine on for generating electricity only. As the fringe fitting fails for T = 20 ms under this condition, we can only use T = 10 ms and T = 5 ms for gravity measurement with our gravimeter. For T = 10 ms, the standard deviation can only reach 3 mGal with an average time of 100 s after correction, which is 2 times bigger than that shown in Figure 5 (b), mainly due to the vibrations induced by the engine. Figure 7 illustrates the result measured when the vehicle moved with a speed of 7 km/h. Only T = 5 ms can be used in this harsh environment. With respect to the experiments mentioned above, the fringe fitting results show that the delay τ_z is always around 2.2 ms. The contribution η_x and η_y, however, vary between -1.5% and 1.1%, which indicates the cross couplings due to the misalignment are very small.

Preprints (www.preprints.org) | NOT PEER-REVIEWED | Posted: 15 November 2021 doi:10.20944/preprints202111.0255.v1

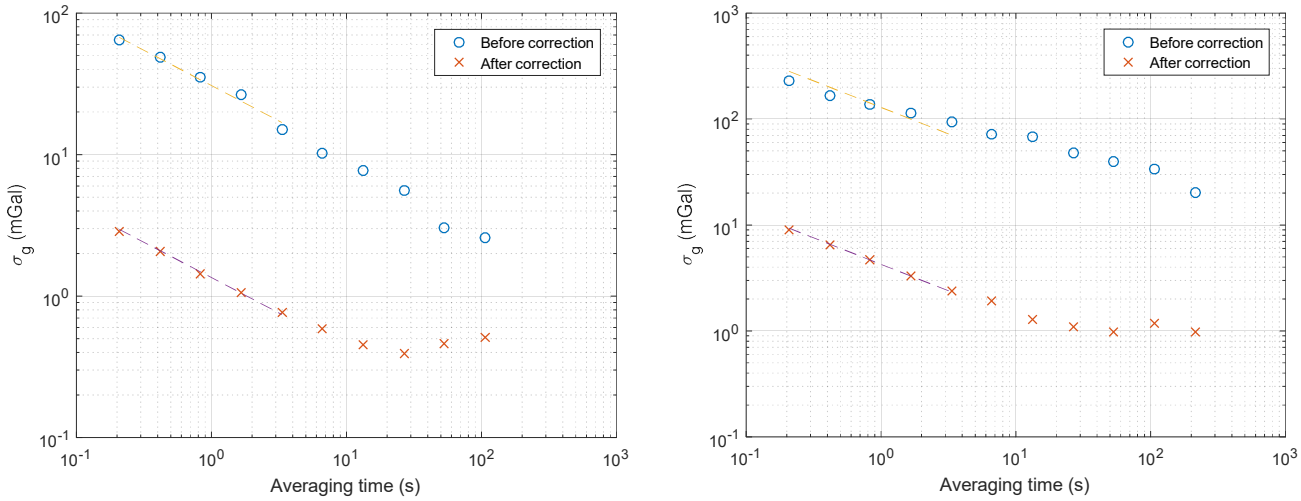

Figure 5. The Allan standard deviation of the gravitational acceleration measured with the vehicle's engine off. (**a**) T = 20ms; (**b**) T = 10 ms.

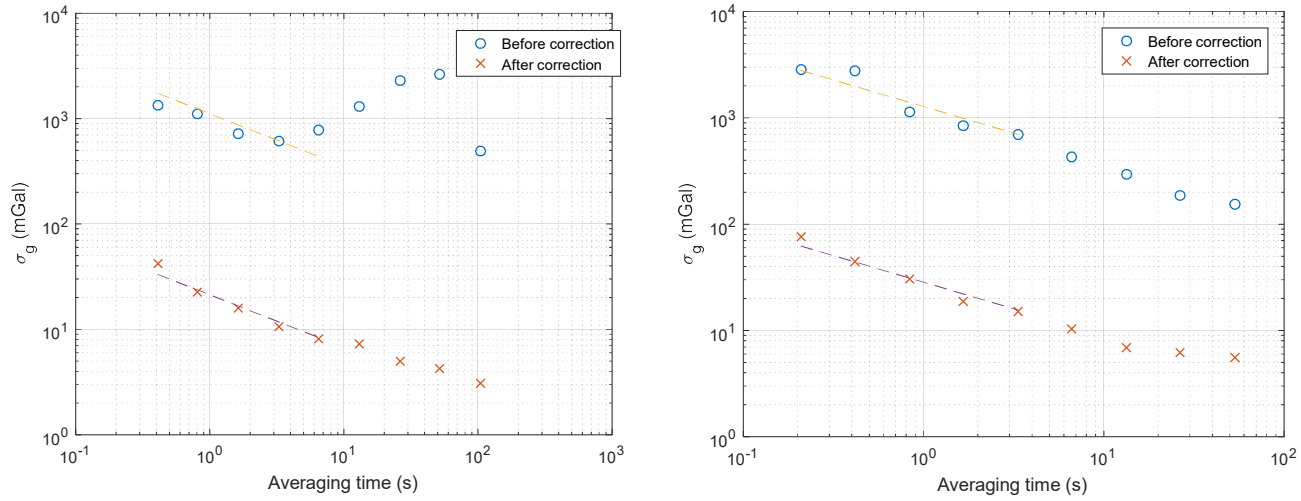

Figure 6. The Allan standard deviation of the gravitational acceleration measured with the vehicle's engine on for generating electricity only. (**a**) T = 10ms; (**b**) T = 5 ms.

Preprints (www.preprints.org) | NOT PEER-REVIEWED | Posted: 15 November 2021 doi:10.20944/preprints202111.0255.v1

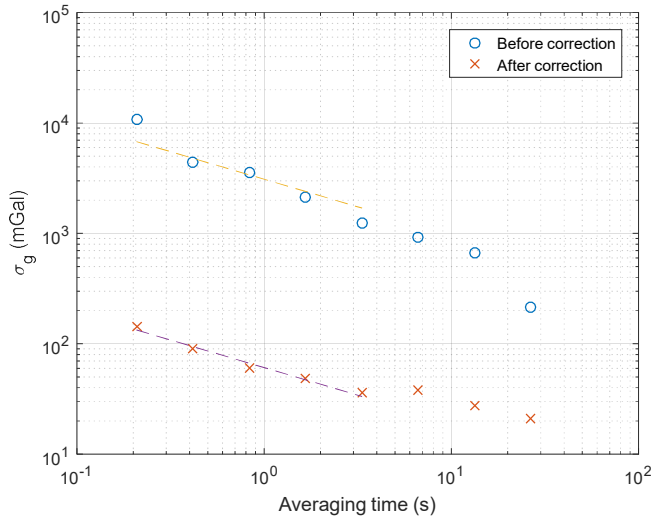

Figure 7. The Allan standard deviation of the gravitational acceleration measured when the vehicle moved with a speed of 7 km/h.

The first 5 points of the curves shown in Figure 5, 6 and 7 display a classical white noise behavior, which is characterized by a linear decrease with a slope of −1/2 in the log-log plot. Therefore, the sensitivity of the gravimeter under various conditions can be calculated by linear regression. The results are listed in Table 3, and shown with the dash lines in Figure 5, 6 and 7. We can use the suppression factor S_1/S_2 to evaluate the post correction, where S_1 is the sensitivity before correction, and S_2 is the sensitivity after correction. The standard deviations of the vibration induced phase noise $\sigma_{\Phi_{vib}}^{rms}$ are also listed in Table 3, which agree with the data shown in Table 2.

Table 3. The sensitivity and suppression factor achieved in various experimental conditions.

Engine	Speed (km/h)	Interrogation time T (ms)	Vibration induced phase noise $\sigma_{\Phi_{vib}}^{rms}$	Sensitivity before correction S_1 (mGal/Hz$^{1/2}$)	Sensitivity after correction S_2 (mGal/Hz$^{1/2}$)	Suppression Factor S_1/S_2
Off	0	20	1.36π	30.76	1.35	22.74
Off	0	10	1.35π	128.83	4.26	30.27
On	0	10	16.70π	1112.08	21.29	52.25
On	0	5	3.99π	1279.44	28.44	44.98
On	7	5	11.53π	3095.66	60.88	50.85

In the moving test, a suppression factor of 50.85 can be achieved, which improves the sensitivity to 60.88 mGal/Hz$^{1/2}$. As the gravity may vary with the position of the vehicle, which is not corrected in the calculation of the Allan standard deviation, we can only use the sensitivity after the vibration noise correction to estimate the precision of the gravimeter. With an averaging time of 100 s, the precision of the gravimeter may reach 6 mGal after the vibration noise correction.

4. Conclusions

A vibration compensation method for atom gravimeters has been summarized in this paper. We have demonstrated that this method can be used for our vehicle-mounted atom gravimeter, though the standard deviation of the vibration induced phase can be as

large as 16.70π. The vertical vibration noise measured with the vehicle engine off is 3 times larger than that in the lab during daytime. In this static condition, we managed to achieve a sensitivity of 1.35 mGal/Hz$^{1/2}$ and a suppression factor of 22.74 with T = 20 ms after the vibration noise correction. And with an average time of 10 s, the standard deviation of the measured gravity data can reach 0.5 mGal. When the vehicle moves with a speed of 7 km/h, the vibration noise in the vehicle can be 2 order of magnitude greater than that in the lab. In this condition, a suppression factor of 50.85 and a sensitivity of 60.88 mGal/Hz$^{1/2}$ were realized with T = 5 ms after the vibration compensation, which makes it possible to measure gravity continuously while the vehicle is moving. To our knowledge, this might be the first report about testing the atom gravimeter in a moving vehicle.

Author Contributions: Conceptualization, J.G. and D.P.; data curation, S.M.; formal analysis, C.Z.; methodology and validation, J.L. and J.G.; resources, B.W.; supervision, H.M. and C.Z.; writing—original draft, J.G.; writing—review & editing, J. L. All authors have read and agreed to the published version of the manuscript.

Funding: This research received no external funding.

Institutional Review Board Statement: Not applicable.

Informed Consent Statement: Not applicable.

Data Availability Statement: The data presented in this study are available on request from the corresponding author.

Acknowledgments: We thank the staff in our laboratory, Xinwen Chen and Fan Guo, et al, for their help with circuit analysis.

Conflicts of Interest: The authors declare no conflict of interest.

References

1. Wu, X.; Pagel, Z.; Malek, B.S.; Nguyen, T.H.; Zi, F.; Scheirer, D.S.; Müller, H. Gravity surveys using a mobile atom interferometer. *Sci. Adv.* **2019,** *5*, eaax0800.
2. Fu, Z.; Wang, Q.; Wang, Z.; Wu, B.; Cheng, B.; Lin, Q. Participation in the absolute gravity comparison with a compact cold atom gravimeter. *Chin. Opt. Lett.* **2019,** *17*, 011204.
3. Hu, D.; Wang, Y.; Ma, H.; Ru, N.; Zhang, L. Gravity acceleration measurement based on atom interferometry. *J. Phys.: Conf. Ser.* **2018,** *1149*, 012021.
4. Kasevich, M.; Chu, S. Atomic interferometry using stimulated Raman transitions. *Phys. Rev. Lett.* **1991,** *67*, 181-184.
5. Gravimeter. Available online: https://aosense.com/product/gravimeter/ (accessed on 17 10 2021).
6. Absolute quantum gravimeter. Available online: https://www.muquans.com/product/absolute-quantum-gravimeter/ (accessed on 17 10 2021).
7. Bidel, Y.; Zahzam, N.; Bresson, A.; Blanchard, C.; Cadoret, M.; Olesen, A.V.; Forsberg, R. Absolute airborne gravimetry with a cold atom sensor. *J. Geod.* **2020,** *94*, 20.
8. Bidel, Y.; Zahzam, N.; Blanchard, C.; Bonnin, A.; Cadoret, M.; Bresson, A.; Rouxel, D.; Lequentrec-Lalancette, M.F. Absolute marine gravimetry with matter-wave interferometry. *Nat. Commun.* **2018,** *9*, 627.
9. Xu, A.; Kong, D.; Fu, Z.; Wang, Z.; Lin, Q. Vibration compensation of an atom gravimeter. *Chin. Opt. Lett.* **2019,** *17*, 070201.
10. Le Gouët, J.; Mehlstäubler, T.E.; Kim, J.; Merlet, S.; Clairon, A.; Landragin, A.; Pereira Dos Santos, F. Limits to the sensitivity of a low noise compact atomic gravimeter. *Appl. Phys. B* **2008,** *92*, 133-144.
11. Peters, A.; Chung, K.Y.; Chu, S. High-precision gravity measurements using atom interferometry. *Metrologia* **2001,** *38*, 25-61.
12. Merlet, S.; Le Gouët, J.; Bodart, Q.; Clairon A.; Landragin, A.; Pereira Dos Santos, F.; Rouchon, P. Operating an atom interferometer beyond its linear range. *Metrologia* **2009,** *46*, 87-94.
13. Ménoret, V.; Vermeulen, P.; Le Moigne, N.; Bonvalot, S.; Bouyer, P.; Landragin, A.; Desruelle, B. Gravity measurements below 10^{-9} g with a transportable absolute quantum gravimeter. *Sci. Rep.* **2018,** *8*, 12300.
14. Richardson, L.L. Inertial Noise Post-Correction in Atom Interferometers Measuring the Local Gravitational Acceleration. PhD Thesis, Gottfried Wilhelm Leibniz Universität, Hannover, 16.01.2019.
15. Zhang, N.; Hu, Q.; Wang, Q.; Ji, Q.; Zhao, W.; Wei, R.; Wang, Y. Michelson laser interferometer-based vibration noise contribution measurement method for cold atom interferometry gravimeter. *Chin. Phys. B* **2020,** *29*, 070601.
16. Wu, B.; Zhou, Y.; Cheng, B.; Zhu, D.; Wang, K.; Zhu, X.; Chen, P.; Weng, K.; Yang, Q.; Lin, J.; Zhang, K.; Wang, H.; Lin, Q. Static measurement of absolute gravity in truck based on atomic gravimeter. *Acta Phys. Sin.* **2020,** *69*, 060302.

17. Zhu, L. A Cold Atoms Gravimeter for Use in Absolute Gravity Comparisons. PhD Thesis, University of Birmingham, Birmingham, 01.2018.
18. Cheinet, P.; Canuel, B.; Pereira Dos Santos, F.; Gauguet, A.; Yver-Leduc, F.; Landragin, A. Measurement of the sensitivity function in time-domain atomic interferometer. *IEEE Trans. Instrum. Meas.* **2008,** *57*, 1141-1148.
19. Geiger, R.; Ménoret, V.; Stern, G.; Zahzam N.; Cheinet, P.; Battelier, B.; Villing, A.; Moron, F.; Lours, M.; Bidel, Y.; Bresson, A.; Landragin, A.; Bouyer, P. Detecting inertial effects with airborne matter-wave interferometry. *Nat. Commun.* **2011,** *2*, 474.
20. Tröbs, M.; Heinzel, G. Improved spectrum estimation from digitized time series on a logarithmic frequency axis. *Measurement* **2006,** *39*, 120-129.
21. Tröbs, M.; Heinzel, G. Corrigendum to "Improved spectrum estimation from digitized time series on a logarithmic frequency axis" [Measurement 39 (2006) 120-129]. *Measurement* **2009,** *42*, 170.